Numerical Assessment of Pavement Test Sections

T. KRAUTHAMMER AND H. KHANLARZADEH

A numerical study was performed at the University of Minnesota for the Minnesota Department of Transportation for assessing and explaining the observed performance of several highway pavement test sections. The test sections that were considered in this study are located in Minnesota near Rothsay, on I-94, and near Olivia, on Trunk Highway 71. For the Olivia site, the objective was to investigate the effect of a thin layer of bituminous bond breaker on the reflective cracking of the new pavement slab, whereas for the Rothsay site the goal was to understand the differences between bituminous-treated bases (BTBs), cement-treated bases (CTBs), and aggregate bases in affecting the pavement behavior and to determine the causes for a relatively poor behavior of pavements on BTBs as compared to pavements on CTBs and aggregate bases. The approach was to use the finite element method and to perform falling-weight deflectometer (FWD) simulations on the test sections. The results from those simulations were compared to FWD test data for model correlation, and finally parametric studies were performed in order to assess the long-term behavior of the pavements under consideration. As a result of the study, preliminary relationships were derived between stress ratios and pavement properties that could affect the long-term pavement behavior. Based on these results, it was possible to provide rational explanations of observed pavement conditions, and to draw significant conclusions on improved procedures for pavement rehabilitation.

This paper is based on a recent study at the Department of Civil and Mineral Engineering at the University of Minnesota for the Minnesota Department of Transportation (MNDOT) in which the performance of several pavement test sections was assessed *(1)*. The general objective of the study was to assist MNDOT to develop optimal methods for rehabilitation of the highway system under its jurisdiction. Two test section sites were considered, one located in the northwestern part of the state on I-94 near Rothsay and the second near Olivia on Trunk Highway (TH) 71 in the southwestern part of the state. At Rothsay, the effect of various types of base materials and thickness on the pavement performance was studied. At the Olivia site in 1977, a 5.5-in. concrete slab over a 1-in. bituminous interlayer as bond breaker was placed on a tapered concrete pavement constructed in 1947. The original pavement consisted of a 22-ft-wide slab, 9 in. thick at the edge and 7 in. thick at the center. The purpose of this test section was to investigate the effect of a bituminous bond breaker on the reflective cracking of the new slab. No further cracking of the old slab was done before placing the new pavement, and after a pavement survey in 1984 it was concluded that virtually no distress existed after nearly 7 years of service. At the Rothsay site, test sections with bituminous-treated bases (BTBs) have performed rather poorly as compared to other sections with aggregate bases or cement-treated bases (CTBs). The purpose of this analytical study was to assist MNDOT in determining the causes for the observed pavement behavior by using an analytical approach based on the finite element method.

Department of Civil and Mineral Engineering, University of Minnesota, 500 Pillsbury Drive S.E., Minneapolis, Minn. 55455.

Previous studies on the analysis of concrete pavement slabs included the work by Chou *(2, 3)* in which the development of a finite element approach for such analyses was described and demonstrated, including the consideration of pavement joint behavior on the slab response. Other researchers also used the finite element method for studying pavement performance and the relationships to design applications. Huang and Wang *(4)* used the modulus of subgrade reaction k obtained from the plate load test for the subgrade characterization, an approach similar to procedures in other studies *(2)*. Tabatabaie and Barenberg *(5, 6)* reported on the development and validation of a finite element code that used a Winkler-type subgrade for studying two-layered cracked pavement sections, including shear transfer across joints or cracks due to aggregate interlock or dowel action. There, too, the initial assumption about the modulus of subgrade reaction was similar to that reported by Chou *(2)* and Huang and Wang *(4)*, but it was later modified by Ioannidis et al. *(7)* who used the concept of the resilient modulus of subgrade reaction K_R, which was based on the subgrade response characterization under repeated impulsive loads.

Extensive information on the finite element method used in this study can be found in books, for example, by Bathe *(8)*. For this study, it was decided to use the commercially available finite element code ADINA *(9)*, which is generally similar to other available multipurpose finite element codes that could be used in a design office environment. The background information on structural dynamics can be obtained from the book by Newmark and Rosenblueth *(10)*, on reinforced concrete structures from the book by Park and Paulay *(11)*, and on foundation dynamics from the texts by Barkan *(12)*, and by Richart et al. *(13)*. The loading conditions used for the experimental part were generated by the well-known falling-weight deflectometer (FWD) method, as discussed in a recent paper by Boutros et al. *(14)* and in the extensive thesis by Foxworthy *(15)*. These loading conditions were later simulated for the finite element analysis based on complete time histories that were obtained experimentally at the sites by MNDOT personnel.

The load from the FWD system is generated by dropping a mass from a selected height. There are four weight levels of 110, 220, 440, and 660 lb, with drop heights from 0.8 to 15 in. for generating equivalent traffic loads of 1,500 to 24,000 lb, respectively. The load induces deflections in the pavement that are derived by integrating velocity-time histories over the load duration. The FWD system produces loads that can be approxi-

mated by a half-sine wave with a duration of 25 to 30 msec, whereas a truck moving at 50 mph creates a loading pulse with durations of about 100 msec *(14)*. Hoffman *(16)* concluded that a stationary nondestructive testing device cannot simulate accurately moving traffic loads; however, the deflections induced by a moving truck compared well with those measured during an FWD test.

APPROACH

The analytical approach for the present study consisted of applying the finite element method for the numerical analyses of the pavement test sections under consideration and comparing the results with experimental data from FWD tests. Once a reasonable agreement was reached between numerical and experimental data and after possible adjustments of the finite element models, it was assumed that the particular model represented accurately the site conditions, and parametric studies of that site were performed for assessing the pavement behavior under given conditions.

FWD LOAD SIMULATION

In structural analysis, the first step is to identify the loading intensity and loading pattern, or configuration. This step includes determination of whether the load is concentrated or distributed and if it is static or dynamic in character. If a dynamic loading condition is present, the load-time history must be known in order to perform the structural or soil-structure interaction analysis. Therefore, it is of utmost importance to have a clear understanding of the loads affecting the pavement. The primary loading on pavements comes from wheel loads on a tire-pavement contact area, and such loads can be simulated using a deflection-based criterion by the FWD equipment *(14, 15)* in which the load is applied dynamically to the pavement while obtaining deflection measurements. The load applied by the FWD was on a circular area, and the problem had to be addressed in three-dimensional (3-D) space. However, in the present modeling the system was assumed to be two dimensional (2-D), and for this reason it was required to convert a 3-D loading case to an equivalent 2-D loading strip configuration for the purpose of comparing the numerical results to those obtained experimentally, as shown in Figure 1. Using the theory of elastic foundation behavior and assuming equal deflections under the two loading cases, an equivalent pressure load for the 2-D case can be found, as follows:

$$(P_{ST}/P_{CR}) = \sqrt{(A_{CR}/A_{ST})} \times (M_{CR}/M_{ST}) \quad (1)$$

where

P_{ST} = pressure applied to strip footing,
P_{CR} = pressure applied to circular footing,
A_{ST} = area of strip footing (1,728 in.^{2}),
A_{CR} = area of circular footing (110 in.^{2})
M_{ST} = influence factor for strip footing (0.68), and
M_{CR} = influence factor for circular footing (0.96).

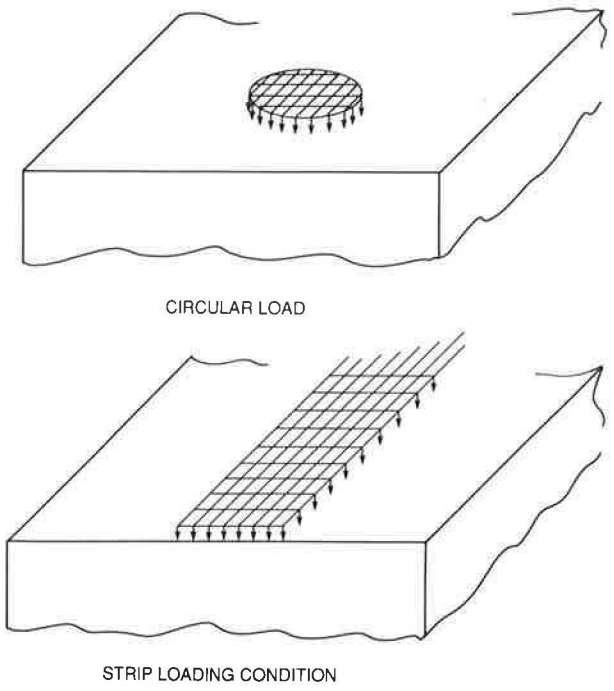

FIGURE 1 3–D versus 2–D loading configurations.

When Equation 1 was applied, it was found that

$$P_{2D} = 0.36P_{3D} \quad (2)$$

In a similar method presented by Bowles *(17)*, the pressure is a function of an influence factor I_W and the least dimension of the footing that leads to a similar solution to the problem.

DAMPING

In dynamic analyses, damping is known to affect the results. Several different methods for obtaining values of damping were examined, for example, those presented by Kuhlemeyer and Lysmer *(18)* and Barkan *(12)*. In order to implement an accurate concept for damping, it was required to obtain a value for a natural frequency of the system ω_n, and to calculate the damping C at each node using the approach proposed by Newmark and Rosenblueth *(10)*, as follows:

$$C = \xi C_{CR} = \xi(2m_E\omega_n) = 2\xi A_E \rho_E \omega_n \quad (3)$$

where

C_{CR} = critical damping of model,
ξ = percent of critical damping,
m_E = mass of the element,
A_E = area of the element, and
ρ_E = mass density of element.

For boundary damping, a value of 100 percent of critical damping was assumed, providing the effect of complete damping in one cycle. For internal nodes, the damping ratios were assumed to be 3, 5, and 7 percent for concrete, asphalt concrete,

and granular materials, respectively. Based on the available information on material properties for the test sites under consideration, the fundamental natural frequencies ω_n were computed with finite element code ADINA *(9)*. The lowest natural frequency of the present model was 1,899 rad/sec for the Rothsay site; this value was inserted into Equation 3 to obtain the damping. The damping was calculated only in the vertical direction because the velocities in the horizontal direction were expected to be small because of the boundary conditions, for which no horizontal motion was allowed. Theoretically, any change in material properties requires the natural frequencies and damping to be recomputed, but it was determined in this study that the largest change in the natural frequency was on the order of 20 percent, and according to Equation 3 it would have an insignificant effect on the nodal damping values. The preceding value for the natural frequency was used to compute the damping and the percentage of the critical damping at every node as required for the ADINA finite element program.

SITE INFORMATION

Rothsay

Twelve test sections with the following properties are located on I-94 near Rothsay, Minnesota.

For the 8-in. slab: dowel diameter = 1 in.; dowel length = 18 in.; dowel spacing = 12 in.; yield strength f_y = 60 ksi. For the 9-in. slab: dowel diameter = 1.25 in.; dowel length = 18 in.; dowel spacing = 12 in. Joints Type C1 were undoweled (first 25 joints in the northern part of each section), whereas joints Type C4 were doweled. Temperature reinforcement, according to AASHTO M55 or M2: dimensions 11 × 18 ft; wire fabric 12 × 6 ft mesh D25 × W23, with f_y = 70 ksi. Tie bars: $^5/_8$ in. in diameter, 30 in. long, and 36 in. of spacing for the L1 joint.

Slab thicknesses: 8 and 9 in.; concrete uniaxial compressive strengths f_C' were from about 3,000 to 7,000 psi with a mean value of 4,944 psi. Slab dimensions: 27 × 12 ft; base thicknesses 5 and 6 in.; base static modulus 15 to 3,000 ksi; and subgrade static modulus 7 to 35 ksi.

Olivia

Test sections were located on TH 71 where 5.5-in.-thick concrete slabs were placed in 1977 over a tapered concrete pavement constructed in 1947. The old pavement consisted of slabs 22 ft wide and 9 in. thick at the edge and 7 in. thick at the center. A 1-in. thickness of bituminous interlayer was placed between the old and the new slabs to serve as bond breaker. The material properties of that site were not well known at the initiation of this study; therefore, a parametric assessment had to be conducted to obtain an accurate set of material properties. The procedure used for this purpose was to simulate FWD tests for the site numerically, to compute the pavement responses for various site conditions, and to determine the site properties from a comparison with experimental data. This approach yielded the following set of material properties, assumed to closely represent those of the actual site conditions, for the present model.

Overlay slab: thickness t_C = 5.5 in.; modulus of elasticity $E_C = 4.5 \times 10^6$ psi; and Poisson ratio $\nu = 0.17$. Bituminous bond breaker: thickness, t_{AC} = 1 in.; E_{AC} = 400 ksi; $\nu = 0.40$. Old slab: thickness, t_{OC} = 8 in. (on average); $E_C = 4.5 \times 10^6$ psi; $\nu = 0.17$. Subgrade soil: thickness t_{SG} = 20 in.; E_{SG} = 140 ksi; $\nu = 0.35$.

THE FINITE ELEMENT MODELS

Rothsay

The model was 64 in. long and had fixed boundaries at the sides and at the bottom, as shown in Figure 2. This finite element mesh consisted of 240 quadrilateral 2-D elements mostly with 4 nodes and 16 quadrilateral elements each having 5 nodes. The mesh was formed to accommodate changes in the thickness of various layers while keeping the element dimension aspect ratios within the 2:1 range. For ease of manipulation and reduction of the computation time, the mesh was divided into 9 element groups. Element Groups 1–4 covered the concrete (32 elements each), Groups 5 and 6 the base (32

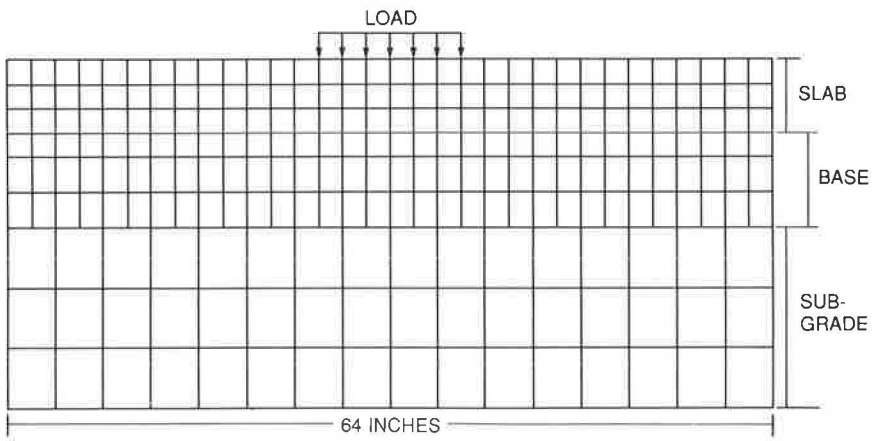

FIGURE 2 Rothsay FE model with element groups.

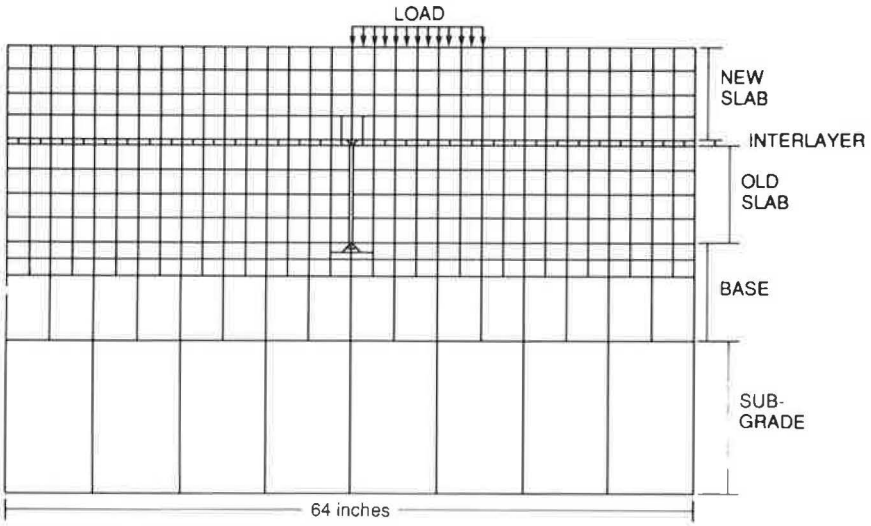

FIGURE 3 Oliva FE model with joint.

elements each), and Groups 7–9 the subgrade soil (16 elements each).

Olivia

This two-dimensional model consisted of 540 nodes with 1,080 degrees of freedom. It was 64 in. long and fixed at its boundaries, as shown in Figure 3. The mesh was divided into 14 element groups in order to reduce computation time as well as for ease of changing layer properties, as follows: 4 element groups for the concrete overlay, 2 for the interlayer (bond breaker), 4 for the old slab, and 4 for the soil. All element dimensions were restricted not to exceed the 2:1 aspect ratio. One joint with an opening of 0.2 in. was introduced at the middle of the old slab with no shear transfer capacity in order to represent an advanced damaged condition.

One of the issues that was addressed during the development of the finite element model was related to the determination of the depth under the pavement that had to be considered in the analysis. Normally, this depth can be determined by computing the distance that a wave would travel in the known simulation time (about 30 msec for the FWD test) from the known seismic velocities of the corresponding materials. Because the seismic wave speed in the present subgrade material is about 2,000 ft/sec, a depth of about 60 ft would be required in the model. This value is not a practical one, and therefore, most of the required 60 ft could be replaced with linear springs having the same stiffness. When this replacement is combined with nonreflecting boundary conditions that can eliminate artificial wave reflections from the model boundaries, the simulation of the problem is expected to be accurate. Furthermore, in the present case the aim was to understand the pavement response as affected by the base material; therefore, although the model considers only changes in the pavement and base, if the subgrade simulation is maintained the same for each site, it may be expected that the relative responses would represent the observed site conditions.

RESULTS

Rothsay Test Sections

Because the elastic properties of concrete, aggregate, soil, and treated bases exhibited a range of values depending on the state of stresses, temperature, compositions, and so forth, the exact properties of the pavement layer at the time of the FWD tests were not known. As a result, an attempt was made to converge numerically to these material properties by performing the numerically simulated FWD tests with the finite element code. Several ranges of these values were tried until both analytical deflection (under the center of applied load) and measured deflection (at the center of the loading plate and at the middle of the slab) were in good agreement. At that time, it was assumed that the material properties that corresponded to the closest numerical values would represent a reasonable approximation of the real site conditions. One of the test sections was chosen for verifying the material properties for this site, and for that section the average measured deflection was equal to 6.22 milli-in., whereas the computed deflection was equal to 6.3 milli-in. for the following material combination: slab thickness $t_C = 9$ in.; $E_C = 5 \times 10^6$ psi; aggregate base thickness $t_{AGG} = 6$ in.; $E_B = 25 \times 10^4$ psi (including dynamic enhancement); subgrade thickness $t_{SG} = 10$ in.; and $E_{SG} = 14 \times 10^4$ psi. Once the site properties were chosen, it was possible to perform a parametric study for assessing the causes for the observed site performance *(19, 20, 22)*.

The criteria selected for assessing the concrete pavement performance were related to the concrete behavior under fatigue conditions. It is an established fact that the concrete fatigue life is a function of the tensile stress ratio (as will be further defined herein). It was shown *(19)* that when this ratio was under 0.55 the concrete could endure virtually an unlimited number of stress repetitions. A similar assumption was adopted for the shear stress ratio, and conclusions regarding the pavement behavior were based on these criteria. The objective of selecting a number of variations of layer thicknesses and

their elastic properties was to examine their effect on the maximum stresses produced by the application of numerically simulated FWD loads.

The variation of the layer properties considered here was in the following range: thickness of concrete slab 8 and 9 in.; concrete modulus of elasticity 4×10^6 and 5×10^6 psi; base thickness 5 and 6 in.; base dynamic modulus 100 to 4,000 ksi; subgrade thickness 10 in.; and subgrade static elastic modulus 35 to 70 ksi. Based on deflection correlation, selected subgrade thickness and its dynamic modulus were 10 in. and 140 ksi, respectively, kept constant for all test sections. Therefore, only four variables were left to be considered, as follows:

1. Concrete thickness t_C (2 values),
2. Concrete modulus of elasticity E_c (2 values),
3. Base thickness t_B (2 values), and
4. Base elastic modulus E_B (100, 150, 250, 300, 500, 750, 1,000, 1,500, 2,000, 2,500, 3,000, 3,500, and 4,000 ksi).

This set of variables brought the total number of combinations to $2 \times 2 \times 2 \times 13 = 104$. However, Variables 1 and 3 (concrete and base thicknesses) were independent, and there was one additional constraint placed on E_B, that when 6 in. of base were used, E_B assumed only two values (150 and 250 ksi, representing the aggregate base), but when 5 in. of base were used, only 11 different values of E_B were considered. Taking these constraints into account and using a partial factorial plan *(20)*, 52 combinations remained, but only 39 out of these combinations were considered in this part of the study. These cases were analyzed, and each finite element computation required 130 to 140 sec of CPU time on an IBM 4341.

As was mentioned earlier, two criteria were selected for assessing the pavement performance, as follows:

1. The ratio of maximum tensile stress (σ_{yy}) of the concrete slab to the tensile strength of concrete represented by the modulus of rupture MR, and
2. The ratio of maximum shear stress (σ_{zy}) to the concrete shear strength v_C represented by $3.5\sqrt{F_C'}$.

After the stress ratios and maximum deflections were computed as functions of base moduli, regression analysis was performed to relate each of the stress ratios to the pavement variables. For the data, a linear regression equation produced the best results.

$$Y = a_0 + a_1X_1 + a_2X_2 + a_3X_3 + a_4X_4 \tag{4}$$

For the tensile stress ratio σ_{yy}/MR, the relationship derived was

$$\sigma_{yy}/MR = 0.55839 - 3.3525 \times 10^{-2}\ t_C - 2.9616 \times 10^{-8}\ E_C + 0.1428\ t_B - 2.0975 \times 10^{-7}\ E_B \tag{5}$$

For this relationship, the sample index of correlation was 0.9133 and the standard error was 0.0284; the standard errors of the coefficients were $\sigma_{a0} = 0.5022$, $\sigma_{a1} = 0.0044$, $\sigma_{a2} = 4.4 \times 10^{-8}$, $\sigma_{a3} = 6.21 \times 10^{-8}$, and $\sigma_{a4} = 1.8 \times 10^{-8}$.

For the shear stress ratio σ_{zy}/v_C, the relationship derived was

$$\sigma_{zy}/v_C = 1.0832 - 4.4281 \times 10^{-2}\ t_C - 7.7 \times 10^{-8}\ E_C + 1.85 \times 10^{-2}\ t_B + 7.6322 \times 10^{-9}\ E_B \tag{6}$$

For this case, the sample index of correlation was 0.8803 with a standard error of 0.0284; the standard errors of the coefficients were $\sigma_{a0} = 0.0946$, $\sigma_{a1} = 0.00826$, $\sigma_{a2} = 8.273 \times 10^{-9}$, $\sigma_{a3} = 1.1698 \times 10^{-2}$, and $\sigma_{a4} = 3.391 \times 10^{-9}$.

The present relationships are in a preliminary form, representing an attempt to verify whether the approach leads to useful results. These are purely descriptive equations and the standard error of the coefficients should not be interpreted in a usual statistical sense because of the fact that the random sampling assumptions were not met. The two relationships represent the effects of changes in any one of four variables on the stress ratios, and may have many useful applications in the future, but only after a more fundamental statistical study is performed. In their modified form, such relationships could be

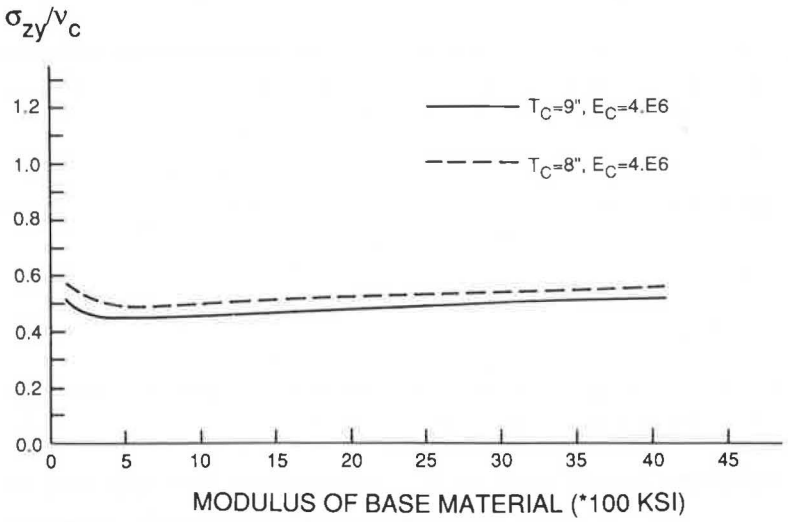

FIGURE 4 Shear stress ratios for various base materials and lower concrete strength.

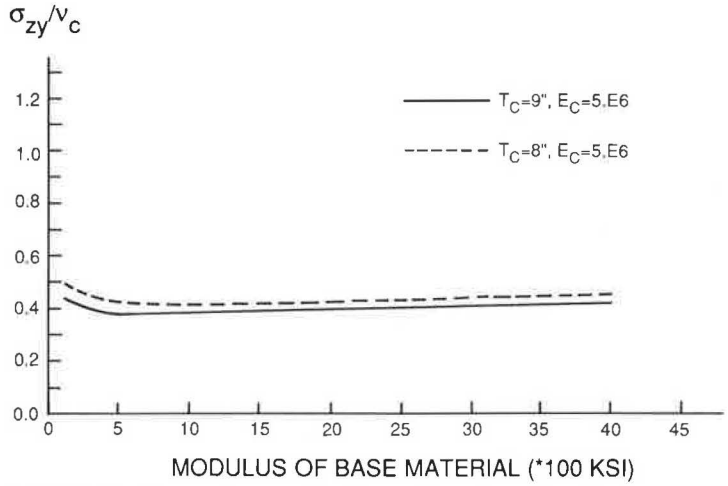

FIGURE 5 Shear stress ratios for various base materials and higher concrete stregth.

used to relate pavement life to the traffic data by using, for example, the Portland Cement Association procedure in which the number and intensity of traffic loads are related to the fatigue life of the pavement system. They may also be used for deriving equivalency factors to convert one type of material to another. For example, one may wish to know for a given pavement life how many inches of a base material could be replaced by 1 in. of concrete slab, and vice versa. However, the use of these equations is not recommended until a complete statistical combination of pavement layer properties is included in the analysis, because equations of this type are considered adequate only when the sample index of correlation is not lower than 0.95. For the present relationship, values were 0.9133 and 0.8803.

As shown in Figure 4 and 5, the shear stress ratio seldom exceeds the value 0.55. This value was attained only once, when slab thickness was 8 in., concrete modulus 4×10^6 psi, and base modulus ≤200 ksi; consequently, one should pay more attention to the tensile stress ratio. Plots of maximum tensile stress over modulus of rupture versus base elastic dynamic modulus, as presented in Figures 6 and 7, revealed that when the dynamic modulus of the base was larger than 900 ksi, the stress ratio was smaller than 0.55; therefore, the pavement slabs should be able to endure virtually an unlimited number of load repetitions.

CTBs normally have moduli in excess of 900 ksi (the range of CTB moduli is 1,000 to 34,000 ksi under static loading conditions); therefore, there should not be a considerable slab deterioration due to base support values. On the other hand, BTBs normally exhibit support moduli in the range of 100 to 2,000 ksi, depending on the mix composition and temperature. Typical values of BTB moduli are 400 to 500 ksi. This range is particularly important during hot summers when BTB moduli decrease to their lower values. In the late spring and early summer, there could be large temperature differentials between day and night. When the base is warm while the top slab

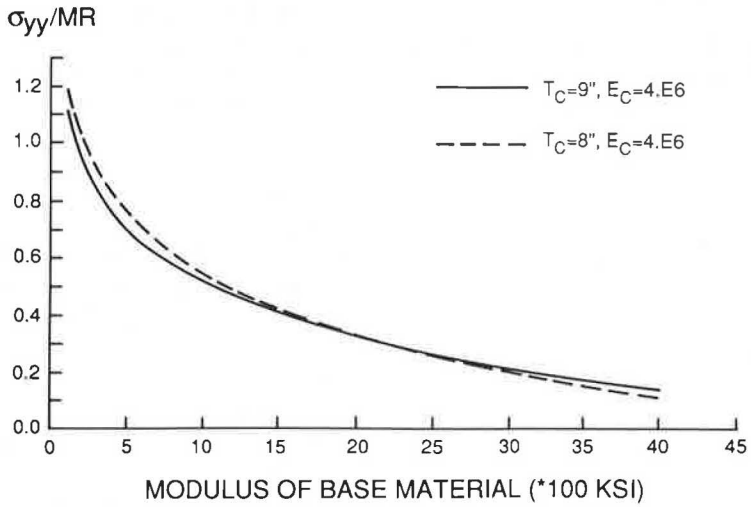

FIGURE 6 Tensile stress ratio for various base materials and lower concrete strength.

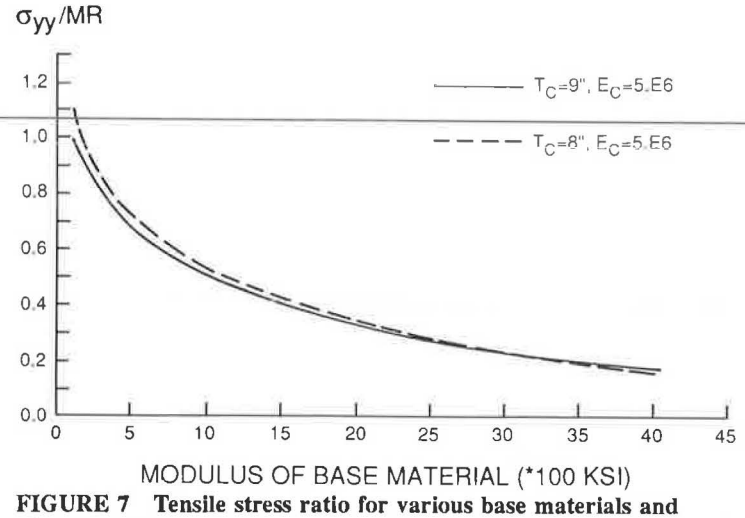

FIGURE 7 Tensile stress ratio for various base materials and higher concrete strength.

surface is cold, the temperature gradient across the thickness of the slab causes the slab to curl up and produces tensile stresses at the top of the slab. At the same time, the base retains a higher temperature, hence, a low modulus. When the traffic load is applied to the pavement as shown in Figures 8a and 8b, the combination of curling stress and loading stresses may cause enhanced stresses along a line parallel to the traffic flow in the slab central region, cracking the slab. This type of crack was observed at the Rothsay test site where the slab was constructed over BTBs. Because the stresses induced by the traffic loads at the surface of the slab tended to be higher for lower base moduli, it became clear that the warmer the base the more severe would be the damage. For example, it was observed from the present results that when E_B was 100 ksi the peak tensile stress at the surface of the slab was 709 psi, whereas when E_B was 1,000 ksi the stress was only 417.9 psi.

The results shown in Figures 6 and 7 suggest that the benefit of a thicker slab diminishes as the base support value increases. For example, increasing the slab thickness from 8 to 9 in. (an increase of 12.5 percent) results in a decrease of about 9 percent in the tensile stress ratio for $E_B \leq 100$ ksi, whereas the same change in slab thickness decreases the stress ratio only by 3.6 percent when E_B is about 850 ksi. The beneficial effect of the thicker slab continuously decreases as the base modulus increases and totally vanishes when E_B is about 1,800 ksi. From this point on, there is a negative effect on the tensile stress ratio as a result of increasing the slab thickness. This phenomenon can be explained by using the theory of beams on elastic foundations *(21)* in which a plot of the tensile stress in the beam as a function of the base reaction modulus for various beam thicknesses yields curves that are not parallel to each other. Therefore, locations on these curves can be defined where increasing the beam thickness results in an increase of the tensile stress for a given base material.

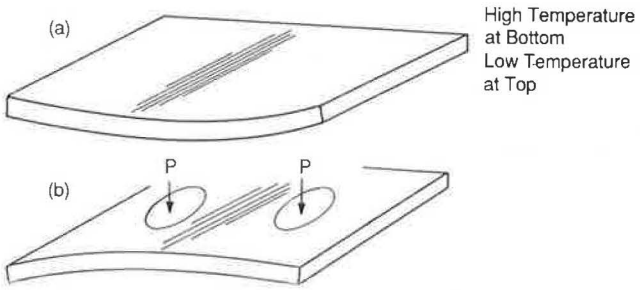

FIGURE 8 Combination of (a) curling effects and (b) traffic loads.

Olivia Test Section

The goal of this part of the analytical study was to investigate the effectiveness of the rehabilitation procedure that had been used, and to demonstrate qualitatively how changes in slab and bond breaker thicknesses and their elastic properties in overlaying materials affect the stresses in the pavement and its long-term behavior. For this task, an approach similar to that used at the Rothsay site was adopted. The preliminary frequency analysis was performed, the natural frequencies were determined, and the fundamental natural frequency (2,580 rad/sec) was used for the damping computations. After the finite element mesh was updated accordingly, the maximum deflection at the center of the slab was computed and compared to the measured data obtained by FWD tests for the same location. Elastic material properties were adjusted until a reasonable match was achieved between the measured and computed deflections. At that point, the model was ready for the parametric analysis in which the old pavement properties were kept constant while changes were made in the thicknesses and material properties of the new slab and the bituminous bond breaker, as follows. New slab thicknesses of 5.5, 6, 7, and 8 in.; bituminous interlayer thicknesses of 0, 0.5, and 1 in.; and bitumen moduli of elasticity of 100, 300, 500, 800, and 1,000 ksi.

A full factorial plan was implemented to account for all combinations of the layer properties, their interaction effects were obtained, and the computations were performed for a total of 33 combinations. (Each computation required about 140 sec of CPU time on an IBM 4341.) The results are presented in

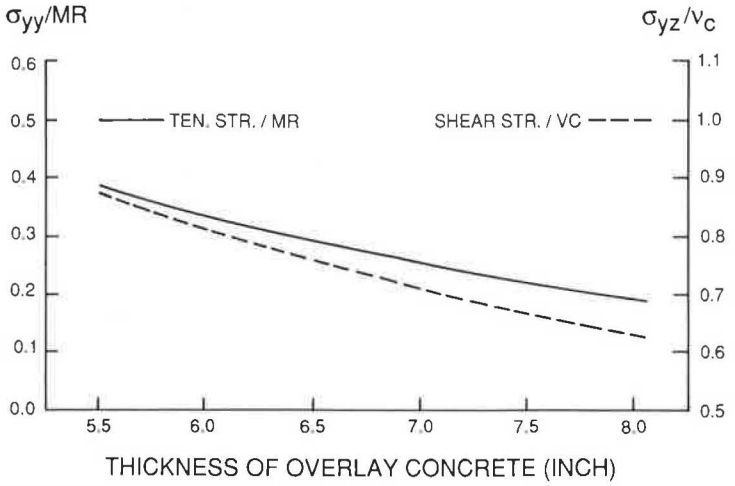

FIGURE 9 Stress ratios without AC interlayer at Oliva.

Figures 9–13. The load was modeled in the same way as were the Rothsay test sections. However, for this section it was determined that the location of the load that produced the most critical stresses was not at the center of the model, but as a result of introducing the pavement joint the critical stresses were obtained when the load was placed next to the joint.

It is shown in Figure 9 that when no bituminous bond breaker was provided the tension stress at the bottom of the new slab was insignificant as far as concrete fatigue was concerned. This result was noticed also in the analysis of the Rothsay site. At Rothsay, it was determined that when the base modulus exceeded 900 ksi the tensile stress ratio at the critical location was less than the fatigue limit of 0.55 at which damage to the concrete would accumulate because of load repetitions. However, at the Olivia site the shear stress ratio for any thickness of new slab was >0.85; therefore, a high shear stress ratio was the dominant factor in determining the life of the structure and the crack propagation when no interlayer was provided.

Change in the tensile stress ratio as a function of overlay thickness and modulus of interlayer is shown in Figure 10. For the thicker slab, the tensile stress ratio was smaller when the modulus of interlayer was 300 ksi or more. Also, the tensile stress ratio under this condition remained less than the 0.55 limit, and should not be of concern even when 1 in. of AC interlayer is provided, as shown in Figure 10. When 1 in. of interlayer bond breaker was provided, the tensile stress ratio exceeded the 0.55 limit only when the interlayer modulus was in the range of up to 150 ksi (Figure 10). This modulus of interlayer is seldom achieved in the northern part of the United States because of the cooler climate. Also, the stresses due to temperature gradient across the slab thickness and those induced by the traffic load tend to cancel part of the tensile stresses at the bottom of the slab. The tensile stress at the top of the slab due to traffic load was limited because of interlayer confinement that resulted in small deflections. When the interlayer thickness was reduced to 0.5 in., the tensile stress ratio

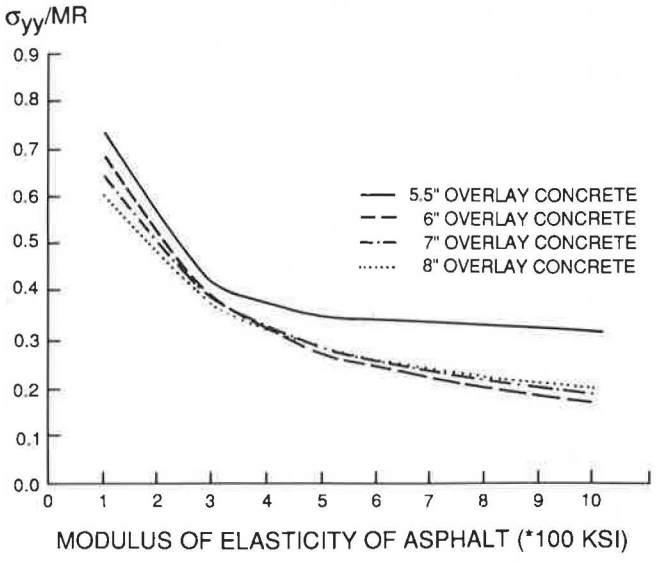

FIGURE 10 Tensile stress ratios for 1.0-in. AC interlayer.

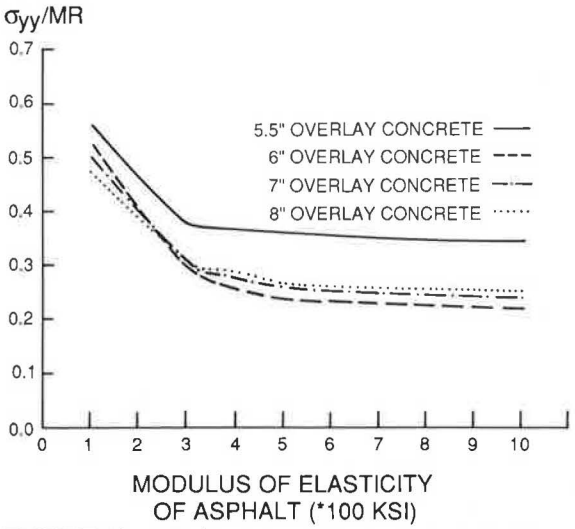

FIGURE 11 Tensile stress ratios for pavement with 0.5 in. of AC interlayer.

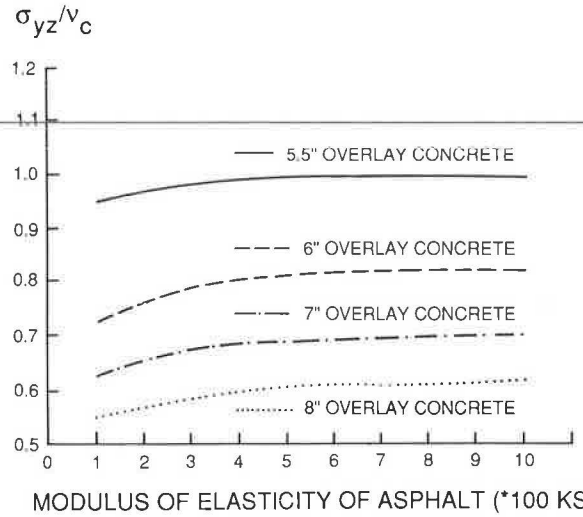

FIGURE 12 Shear stress ratios for pavement with 1.0-in. AC interlayer.

improved as shown in Figure 11. Having a too-thick AC interlayer would increase the tensile stress ratio, so this condition should be assessed for each site during the overlay design.

The modulus of bond breaker and its thickness affected the shear stress ratio as shown in Figures 12 and 13, in which 1 in. of interlayer and 8 in. of concrete slab exhibit a much lower shear stress ratio at every temperature (i.e., at any modulus of interlayer bond breaker), and a greater modulus of interlayer has a small effect on the shear stress ratio when 1 in. of AC interlayer is provided. Under this condition (large E_{AC} and thin interlayer), the effect of bond breaker diminishes and approaches that of no stress relief layer as shown in Figure 9. Therefore, when designing the mix for a stress relief layer, the negative effect of stiff AC mixes on the shear stress ratios should be considered.

All these cases were computed with an open joint; that is, there was no shear transfer across the joint. This assumption may not be correct for all cases, but because the old pavement was assumed to be damaged significantly, it seemed to be justified. Furthermore, any introduction of shear transfer would lead to lower shear stress ratios; thus the present results can be considered to represent relatively more severe pavement damage conditions at the site.

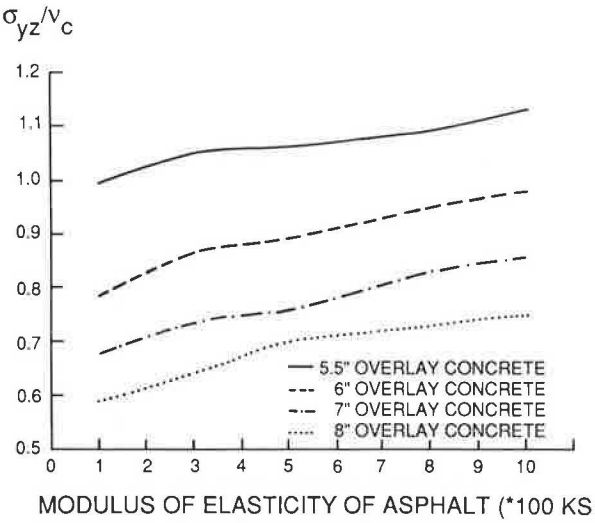

FIGURE 13 Shear stress ratios for pavement with 0.5-in. AC interlayer.

CONCLUSIONS AND RECOMMENDATIONS

The application of the finite element method has been demonstrated for the analysis of layered pavement systems that included several types of materials and site conditions. In this analysis, the loading condition that was used simulated in two dimensions the three-dimensional FWD-induced loads. Special attention was devoted to preserving the dynamic characteristics of the problem and the site geometry. The results obtained appear to be reasonable compared to those reported from previous studies. They compared well with the experimental data and observations at the test sites. Based on the calculated results, the following recommendations were suggested:

1. For a new pavement that may have a low subgrade support, using a cement-treated base for economical crack control is recommended. The experiences gained in Minnesota and Michigan do not support the use of BTBs. When BTBs are deemed to be the only viable option, the designer should take into account the potential temperature differences over various 24-hr periods. When the temperature variation is relatively large, the use of less temperature-susceptible bituminous materials is urged. Also, substantial saving could be realized by providing a thinner slab when CTBs with moduli of 900 ksi or more are used.
2. In overlay design, it appears that the best policy of controlling either tensile- or shear-induced reflective cracking is to provide 1 in. of bituminous interlayer with a small (under 500 ksi) modulus of elasticity as bond breaker.
3. The results of this parametric study suggest that in overlay design tensile stresses are usually of little importance, and that only shear stresses may reach a damaging magnitude. The thicker the slab the less is the shear stress ratio. However, because of economical considerations slabs of more than 7 in. are not constructed; therefore, the interlayer modulus should be decreased as the slab thickness is reduced.

ACKNOWLEDGMENTS

This paper was prepared from a study performed at the Department of Civil and Mineral Engineering, University of Minnesota. The project was sponsored by the Minnesota Department of Transportation (MNDOT) with G. Cochran as project coordinator.

The authors express their appreciation to the personnel at MNDOT for their cooperation and support during this study. The computations were performed on an IBM 4341 at the Department of Civil and Mineral Engineering, University of Minnesota. The authors wish to thank the computer facilities personnel for their cooperation. Also, thanks are due to M. I. Darter and to M. R. Thompson of the University of Illinois at

Urbana for their comments during several discussions on the subject. Finally, the authors wish to thank J. Lin for his assistance.

REFERENCES

1. T. Krauthammer and H. Khanlarzadeh. *Pavement Rehabilitation Evaluation by Analysis of Minnesota Test Sections*. Report ST-86-03. Department of Civil and Mineral Engineering, University of Minnesota, Minneapolis, Aug. 1986.
2. Y. T. Chou. *Structural Analysis Computer Program for Rigid Multicomponent Pavement Structures with Discontinuities—WESLIQID and WESLAYER*. Report GL-81-6, Parts 1–3. U.S. Army Corps of Engineers Waterways Experiment Station, Vicksburg, Miss., May 1981.
3. Y. T. Chou. Stress Analysis of Small Concrete Slabs on Grade. *ASCE Journal of Transportation Engineering*, Vol. 110, No. 5, Sept. 1984, pp. 481–491.
4. Y. Huang and S. T. Wang. Finite Element Analysis of Concrete Slabs and Its Implications for Rigid Pavement Design. In *Highway Research Record 466*, HRB, National Research Council, Washington, D.C., 1973, pp. 55–69.
5. A. M. Tabatabaie and E. J. Barenberg. Finite Element Analysis of Jointed or Cracked Concrete Pavements. In *Transportation Research Record 671*, TRB, National Research Council, Washington, D.C., 1978, pp. 11–19.
6. A. M. Tabatabaie and E. J. Barenberg. Structural Analysis of Concrete Pavement Systems. *ASCE Journal of Transportation Engineering*, Vol. 106, No. TE5, Sept. 1980.
7. A. M. Ioannidis, E. J. Barenberg, and M. R. Thompson. Finite Element Model with Stress Dependent Support. In *Transportation Research Record 954*, TRB, National Research Council, Washington, D.C., 1984, pp. 10–16.
8. K. J. Bathe. *Finite Element Procedures in Engineering Analysis*. Prentice-Hall, Englewood Cliffs, N.J., 1982.
9. *ADINAT: A Finite Element Program for Automatic Dynamic Incremental Nonlinear Analysis*. Report AE 81-1. ADINA Engineering, Watertown, Mass., Sept. 1981.
10. N. M. Newmark and E. Rosenblueth. *Fundamentals of Earthquake Engineering*. Prentice-Hall, Englewood Cliffs, N.J., 1971.
11. R. Park and T. Paulay. *Reinforced Concrete Structures*. John Wiley & Sons, New York, 1975.
12. D. D. Barkan. *Dynamics of Bases and Foundations*. McGraw-Hill, New York, 1962.
13. F. E. Richart, Jr., J. R. Hall, Jr., and R. D. Woods. *Vibrations of Soils and Foundations*. Prentice-Hall, Englewood Cliffs, N.J., 1970.
14. S. Boutrus, T. G. Davis, and M. S. Mamlouk. Dynamics of Falling Weight Deflectometer. *ASCE Journal of Transportation Engineering*, Vol. 111, No. 6, Nov. 1985, pp. 618–632.
15. P. T. Foxworthy. *Concepts for the Development of a Nondestructive Testing and Evaluation System for Rigid Airfield Pavements*. Ph.D. thesis, Department of Civil Engineering, University of Illinois at Urbana-Champaign, June 1985.
16. M. S. Hoffman and M. R. Thompson. Comparative Study of Selected Nondestructive Testing Devices. In *Transportation Research Record 852*, TRB, National Research Council, Washington, D.C., 1982, pp. 32–41.
17. J. E. Bowles. *Foundation Analysis and Design*, 3rd ed. McGraw-Hill, New York, 1982.
18. R. L. Kuhlemeyer and J. Lysmer. Finite Dynamical Model for Infinite Media. *Journal of the Soil Mechanics and Foundations Division*, ASCE, Aug. 1969, pp. 859–877.
19. E. J. Yoder and M. W. Witczak. *Principles of Pavement Design*, 2nd ed. John Wiley & Sons, New York, 1975.
20. W. G. Cochran and G. M. Cox. *Experimental Design*, 2nd ed. John Wiley & Sons, New York, 1957.
21. M. Hetenyi. *Beams on Elastic Foundations*. The University of Michigan Press, Ann Arbor, 1979.
22. H. Lotfi and M. W. Witczak. Dynamic Characterization of Cement-Treated Bases and Subbase Materials. In *Transportation Research Record 1031*, TRB National Research Council, Washington, D.C., 1984, pp. 41–45.

Publication of this paper sponsored by Committee on Pavement Rehabilitation.